

PHYSICS WITH HADRONIC PROBES AT COMPASS

BERNARD KETZER

*Technische Universität München, Physik Department E18,
D-85748 Garching, Germany
Bernhard.Ketzer@ph.tum.de*

FOR THE COMPASS COLLABORATION

This paper describes the methods and goals of the spectroscopy programme of COMPASS using hadron beams, and reports on first results from a short pilot run using a 190 GeV/c pion beam, carried out in 2004. A partial wave analysis of the reaction $\pi^- N \rightarrow \pi^- \pi^- \pi^+ N'$ shows significant production of a state with spin-exotic quantum numbers $J^{PC} = 1^{-+}$ at 1.6 GeV/ c^2 .

Keywords: Hadron structure; hadron spectroscopy; hadron dynamics; light meson spectrum; glueballs; hybrids.

PACS numbers: 13.20.Fc, 13.20.Gd, 14.40.Lb, 29.30.-h

1. Introduction

The goal of the COMPASS experiment at CERN¹ is to obtain a better understanding of the structure and dynamics of hadrons, which are both aspects of non-perturbative Quantum Chromodynamics (QCD), as the strong coupling constant α_s approaches unity for the corresponding length scales of $\sim 10^{-15}$ m. To this end, a rich physics program is conducted covering a wide range of squared momentum transfer Q^2 from a few 10^{-4} GeV $^2/c^2$ up to 10^2 GeV $^2/c^2$. In its first phase between 2002 and 2007, COMPASS studied the nucleon spin structure by deep inelastic scattering of 160 GeV/c muons off a polarised ${}^6\text{LiD}$ or NH_3 target. The second phase of COMPASS, which started in 2008, is dedicated to experiments with hadron beams of up to 280 GeV/c. Of particular interest in the spectroscopy of the light meson sector are states which do not fit into the constituent quark model like glueballs, hybrids, or multi-quark systems. New states have been observed which still lack an unambiguous explanation. In order to gain more insight, experiments with higher statistical accuracy, extending the spectrum to masses beyond 2.2 GeV/c 2 , have to be performed. In addition, Primakoff reactions, i.e. Coulomb scattering of pions or kaons off quasi-real photons from a nuclear target at very small momentum transfers, open the possibility to test effective field theory predictions for fundamental low-energy parameters, such as the polarisabilities of mesons.

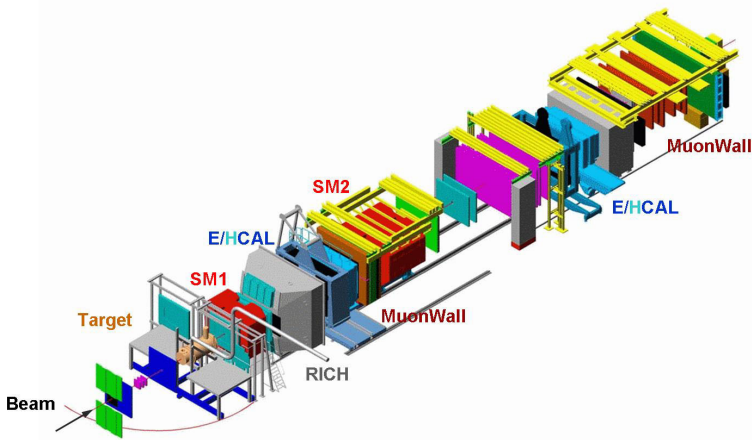


Fig. 1. 3-D view of the COMPASS spectrometer. The total length of the apparatus is about 50 m.

2. The COMPASS Experiment

The COMPASS physics program mentioned above puts high demands both on the beam and on the experimental setup. The Super Proton Synchrotron (SPS) at CERN delivers proton beams, secondary hadron beams (π , K) and tertiary polarised muon beams with momenta between 100 and 300 GeV/c at intensities up to $4 \cdot 10^7$ part./s, as required by the small cross sections of the processes under investigation in the two experimental programmes. Figure 1 shows a schematic view of the experimental setup¹. For the measurements with hadron beams a 40 cm long liquid hydrogen target with a diameter of 35 mm, or simple disks of solid target material are used. The spectrometer has been optimised for large angular acceptance over a broad kinematical range. The tracks of the incoming beam particle and those of the outgoing particles immediately downstream of the target are measured by several planes of scintillating fibre and Silicon microstrip detectors. In order to maximise the momentum acceptance, the spectrometer is equipped with two dipole magnets (SM1 and SM2 in Fig. 1) with field integrals of 1.0 Tm and 4.4 Tm, respectively, both surrounded by tracking detectors of varying granularity and resolution depending on the distance from the beam axis. Particle identification in the momentum range between 5 and 45 GeV/c is performed by a RICH detector. Electromagnetic and hadronic calorimeters (E/HCAL in Fig. 1) are installed in both stages of the spectrometer. Large acceptance electromagnetic calorimetry with high resolution is of particular importance for decay channels involving π^0 , η or η' .

3. Light Meson Spectroscopy with COMPASS

In the simple SU(3)_{flavour} constituent quark model light mesons are described as bound states of a quark q and an antiquark \bar{q}' with quark flavours u, d, s . Mesons are

characterised by their quantum numbers J^{PC} , with the total angular momentum J , the parity P and the charge conjugation parity C . In the quark model they are given by

$$P = (-1)^{L+1}, \quad C = (-1)^{L+S}, \quad (1)$$

where L is the relative orbital angular momentum of q and \bar{q}' and S the total intrinsic spin of the $q\bar{q}'$ pair, with $S = 0, 1$. In addition to J^{PC} the isospin I and the G parity, defined by

$$G = (-1)^{I+L+S} \quad (2)$$

are conserved quantum numbers in strong interactions.

The quark model model has been quite successful in explaining some of the properties of mesons as well as, to a large extent, the observed meson spectrum, even though it makes no assumptions concerning the nature of the binding force, except that hadrons are postulated to be colour singlet states. In QCD, the interaction between coloured quarks is described by the exchange of gluons which carry colour themselves. Owing to this particular structure of QCD, colour-singlet mesons can be composed not only of constituent quarks, but also of other colour-neutral configurations like four-quark objects, and excited (constituent) gluons, which then contribute to the quantum numbers of the hadrons: *hybrids* are resonances consisting of a colour octet $q\bar{q}'$ pair neutralised in colour by an excited gluon, *glueballs* are states composed entirely of excited gluons. Such configurations, however, will mix with ordinary $q\bar{q}'$ states with the same J^{PC} , making it difficult to disentangle the contribution of each configuration. The observation of exotic states with quantum numbers not allowed in the simple quark model, e.g. $J^{PC} = 0^{--}, 0^{+-}, 1^{-+}, \dots$, would give clear evidence for physics beyond the quark model, thus providing a fundamental confirmation of QCD.

The lowest mass glueball has scalar quantum numbers, $J^{PC} = 0^{++}$, and is predicted by LQCD² at a mass of ~ 1.7 GeV/c². The $f_0(1500)$ observed by Crystal Barrel³ and WA102⁴ has been proposed as an experimental candidate for a light glueball, but mixing with ordinary isoscalar $q\bar{q}'$ mesons makes its interpretation difficult. The lowest-lying hybrid, in contrast, is expected⁵ to have exotic quantum numbers $J^{PC} = 1^{-+}$, and thus will not mix with ordinary mesons. Its mass is predicted in the region 1.3–2.2 GeV/c². There are two experimental candidates for a light 1^{-+} hybrid. The $\pi_1(1400)$ was observed by E852⁶ and by VES⁷ in the reaction $\pi^-N \rightarrow \eta\pi^-N$, and by Crystal Barrel^{8,9} in $\bar{p}n \rightarrow \pi^-\pi^0\eta$ and $\bar{p}p \rightarrow 2\pi^0\eta$ Dalitz plot analyses. Another 1^{-+} state, the $\pi_1(1600)$, decaying into $\rho\pi^{10,11}$, $\eta'\pi^{12,13}$, $f_1(1285)\pi^{14,15}$, and $\omega\pi\pi^{16,15}$ was observed in peripheral π^-p interactions in E852 and VES. The resonant nature of both states, however, is still heavily disputed in the community^{17,15}.

COMPASS is expected to shed new light on these questions, by gathering high-statistics samples for final states containing both neutral and charged particles, using π , K, p as projectiles. Two different production mechanisms are employed:

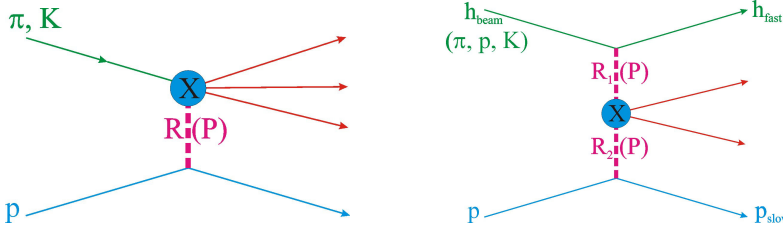


Fig. 2. Mechanisms for meson production studied at COMPASS. (Left) Diffractive dissociation via Reggeon/Pomeron exchange. (Right) Central production via double Reggeon/Pomeron exchange.

diffractive dissociation and central production, which can be described to proceed via the exchange of one or two Reggeons, respectively, between the beam and the target particle. States with gluonic degrees of freedom are generally believed to be enhanced in reactions in which Pomerons, i.e. Reggeons with vacuum quantum numbers, are exchanged.

3.1. Diffractive dissociation

Consider the reaction

$$a + b \longrightarrow c + d \quad , \text{with} \quad c \longrightarrow 1 + 2 + \dots + n \quad , \quad (3)$$

where a is the incoming beam particle, b the target, c the diffractively produced object decaying into n particles, and d the target recoil particle, which stays intact. The reaction proceeds via t -channel exchange of a particle with mass and spin (Reggeon), as indicated in Fig. 2 (left), and is described by 2 kinematical variables: s and $t' = |t| - |t|_{\min}$, where $s = (p_a + p_b)^2$ is the square of the total centre of mass energy and $t = (p_a - p_c)^2$ is the square of the four momentum transferred from the incoming beam to the outgoing system c . The minimum value of $|t|$ which is allowed by kinematics for a given mass m_c is called $|t|_{\min}$. In the overall centre-of-mass frame of the reaction

$$\begin{aligned} t' &= |t| - |t|_{\min} = 2|\vec{p}_a||\vec{p}_c|(1 - \cos\theta_0) \geq 0 \quad , \\ |t|_{\min} &= 2(E_a E_c - |\vec{p}_a||\vec{p}_c|) - m_a^2 - m_c^2 \quad , \end{aligned} \quad (4)$$

where E_i , \vec{p}_i and m_i , $i = a, c$ are the energy, 3-momentum and mass of the beam and the diffractively produced system in the centre-of-mass system, respectively, and θ_0 is the scattering angle.

The total cross section for diffractive reactions is of the order of $1 - 2 \text{ mb}$. In a fixed target experiment like COMPASS, with a $190 \text{ GeV}/c \pi$ beam impinging on a proton target, even states with masses above $3 \text{ GeV}/c^2$ can be produced diffractively, although the differential cross section drops as $1/m_c^2$. Their decay products are emitted mostly at small angles with respect to the incoming beam direction, requiring an extremely good angular resolution.

3.2. Central production

Central production of a resonance X proceeds via the fusion of two Reggeons emitted by the beam and the target particle (Fig. 2 right), which both keep their identity. In the centre of mass frame both beam and target particles lose only a small fraction x_a and x_b of their energy, respectively. At high beam momenta and for small transverse momentum transfer, the mass of the centrally produced system is $m_X = \sqrt{s x_a x_b}$, where s is the squared centre of mass energy. The resonance X carries only a small fraction $x_F = \approx 0$ of the maximum longitudinal centre of mass momentum, with

$$x_F \equiv p_L/p_L^{\max} \approx 2p_L/\sqrt{s} , \quad (5)$$

while x_F is close to 1 for the scattered beam particle and close to -1 for the target particle. In a fixed target experiment, the beam hadron appears as the leading particle in the laboratory system (h_{fast}), whereas the target recoil proton is slow (p_{slow}). The centrally produced system can be identified by a gap in rapidity y to the leading beam or target recoil particle, with

$$y = \frac{1}{2} \ln \left(\frac{E + p_L}{E - p_L} \right) . \quad (6)$$

With a 190 GeV/c π beam scattered off a proton target, masses up to 1.9 GeV/c 2 can be produced centrally for $x_a = x_b = 0.1$. Higher mass states require higher energy losses of beam or target particle, and consequently a less clear separation of central production events from different production mechanisms like single diffraction. With $x_a = 0.2$ and $x_b = 0.1$ masses up to 2.7 GeV/c 2 can be produced, with a rapidity gap to the fast pion of $\Delta y \sim 4.3$ and to the slow proton of $\Delta y \sim 3.3$.

4. Analysis of 3π Production

In order to study the capability of COMPASS to contribute to the field of light meson spectroscopy, diffractive reactions of a 190 GeV/c π^- beam on a lead target were studied in a short pilot run in 2004. The $\pi^- \pi^- \pi^+$ final state was chosen because the disputed $\pi_1(1600)$ meson with exotic J^{PC} quantum numbers had previously been reported in this channel. The trigger selected events with one incoming particle and at least two outgoing charged particles detected in the spectrometer. In the offline analysis, a primary vertex inside the target with 3 outgoing charged particles is required. Since the recoil particle was not detected in 2004, a different procedure is applied in order to select exclusive events where the target stayed intact. The beam energy E_a is calculated from the total energy E_c of the 3π system and the scattering angle θ_0 , assuming that the target particle remained intact throughout the scattering process. Then an exclusivity cut is applied, requiring E_a to be within ± 4 GeV of the nominal beam energy. Figure 3 (left) shows the invariant mass of the corresponding events for all momentum transfers t' (yellow histogram), and for five different ranges in t' . For our further analysis we restrict ourselves to the

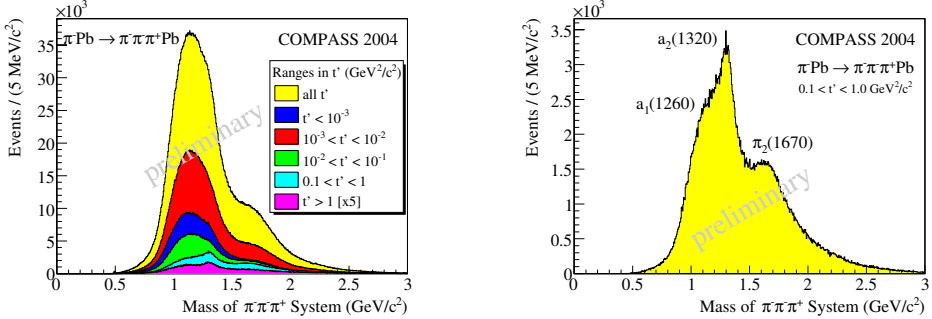


Fig. 3. Invariant mass of the 3π system: (left) for different t' bins; (right) $0.1 \text{ GeV}^2/\text{c}^2 < t' < 1.0 \text{ GeV}^2/\text{c}^2$.

range $0.1 \text{ GeV}^2/\text{c}^2 < |t'| < 1.0 \text{ GeV}^2/\text{c}^2$, shown separately in Fig. 3 (right), where candidates for spin exotic states have been reported in the past. In our sample of 450 000 events, the well-known resonances $a_1(1260)$, $a_2(1320)$, and $\pi_2(1670)$ are clearly visible as bumps in the 3π mass spectrum.

A partial wave analysis (PWA) of this data set was performed using a program which was originally developed at Illinois, and later modified at Protvino and Munich. The reaction is assumed to proceed via t -channel Reggeon exchange at high \sqrt{s} , thus justifying the factorisation of the total cross section into a resonance and a recoil vertex without final state interaction. Since the exchanged Reggeon carries angular momentum, the incident pion ($J^{PC} = 0^{-+}$) may be excited to a state X with different J^{PC} , limited only by conservation laws for strong interactions. For the $(3\pi)^-$ final state $I \leq 1$; we assume $I = 1$ since no flavour-exotic mesons have been found. Since in addition $G = -1$ for a system with an odd number of pions, $C = +1$ follows from eq. (2).

The excited state is then assumed to decay into an isobar and an unpaired (bachelor) pion, followed by the decay of the isobar into two pions. In our analysis we consider the isobars $(\pi\pi)_S$ (including the broad $\sigma(600)$ and $f_0(1370)$), $\rho(770)$, $f_0(980)$, $f_2(1270)$, and $\rho_3(1690)$. The spin-parity composition of the excited state X is studied in the Gottfried-Jackson frame, which is the X centre of mass frame with the z -axis along the beam direction, and the y -axis perpendicular to the production plane, formed by the momentum vectors of the target and the recoil particle.

The PWA is done in two steps. In the first step, a mass-independent fit of angular distributions is performed in $40 \text{ MeV}/c^2$ bins of the 3π invariant mass, where the production strength for a given wave can be assumed to be constant:

$$\sigma_{\text{indep}}(\tau) = \sum_{\epsilon=-1}^1 \sum_{r=1}^{N_r} \left| \sum_i T_{ir}^\epsilon \psi_i^\epsilon(\tau) \right|^2 \quad . \quad (7)$$

Here, T_{ir}^ϵ are the production amplitudes and ψ_i^ϵ the decay amplitudes, the indices i and ϵ denoting different partial waves, characterised by a set of quantum numbers

$J^{PC} M^\epsilon [\text{isobar}] L$, with J^{PC} as defined above; M the absolute value of the spin projection onto the z -axis; ϵ the reflectivity, which describes the symmetry under a reflection at the production plane, and corresponds, at high s , to the naturality of the exchanged Regge trajectory; L is the orbital angular momentum between the isobar and the bachelor pion. The ψ_i^ϵ are constructed based on the isobar model and thus depend on the phase space parameters τ of the 3-body decay, but do not contain any free parameters. Dividing each decay amplitude by its normalisation integral compensates its dependence on m inside each mass bin. The sum contains two non-coherent sums over the reflectivity ϵ and the rank N_r . Assuming that both the target and the recoil particles are nucleons due to the high values of t' considered in this analysis, we set $N_r = 2$, corresponding to helicity-flip and helicity-non-flip amplitudes at the baryon vertex. In addition, the t' dependence of the cross section (especially for $M = 0$ and $M = 1$) is taken into account by multiplying different functions of t' to the decay amplitudes, obtained from the data by making fits in slices of t' . In total 42 partial waves are included in the first step of the fit. It comprises the non-exotic positive reflectivity waves with $J^{PC} = 0^{-+}$ ($M = 0$), $1^{++}, 2^{-+}, 3^{++}, 4^{-+}$ ($M = 0, 1$), $2^{++}, 4^{++}$ ($M = 1$), the exotic 1^{-+} ($M = 1$), and the negative-reflectivity waves $1^{-+}, 2^{++}$ ($M = 0, 1$), $1^{++}, 2^{-+}$ ($M = 1$), taking into account all relevant decay modes of the known resonances. It also contains a background wave, characterised by a uniform distribution in the relevant decay angles, which is added incoherently to the other waves. The sets of complex numbers T_{ir}^ϵ are subject to optimisation using an extended maximum likelihood method, which also takes into account the experimental acceptance of the spectrometer, determined from a Monte Carlo simulation of the apparatus. It is worth stressing that COMPASS has an excellent acceptance for diffractively produced 3π events of the order of 60% over the whole phase space.

In the second step of the PWA a mass-dependent χ^2 fit to the results of the first step is performed, taking into account the mass-dependence of the produced resonances through relativistic Breit-Wigner functions (and possibly a coherent background). In this fit only a subset of seven waves of the first step is used, the selected waves showing either significant amplitudes or rapid phase motions in the $1.6 \text{ GeV}/c^2$ mass range.

Fig. 4 (top) and (bottom left) show the intensities of the three most prominent waves $1^{++} 0^+ \rho\pi S$, $2^{-+} 0^+ f_2\pi S$, and $2^{++} 1^+ \rho\pi D$. The intensity of the exotic $1^{-+} 1^+ \rho\pi P$ wave is shown in Fig. 4 (bottom right, topmost curve). We observe a broad bump in the intensity for this wave centred at $1.6 \text{ GeV}/c^2$, which we interpret as the $\pi_1(1600)$.

The resonance nature of this wave is demonstrated via its phase differences to the two prominent waves shown in Fig. 4 (top), namely $1^{++} 0^+ \rho\pi S$ and $2^{-+} 0^+ f_2\pi S$. The latter, shown in Fig. 5 (right), does not exhibit any significant motion between 1.4 and $1.9 \text{ GeV}/c^2$, which is attributed to the fact there are two resonances, $\pi_1(1600)$ and $\pi_2(1670)$, with very similar masses and widths, causing the relative phase motion to vanish. In contrast to this the phase difference to the 1^{++} wave,

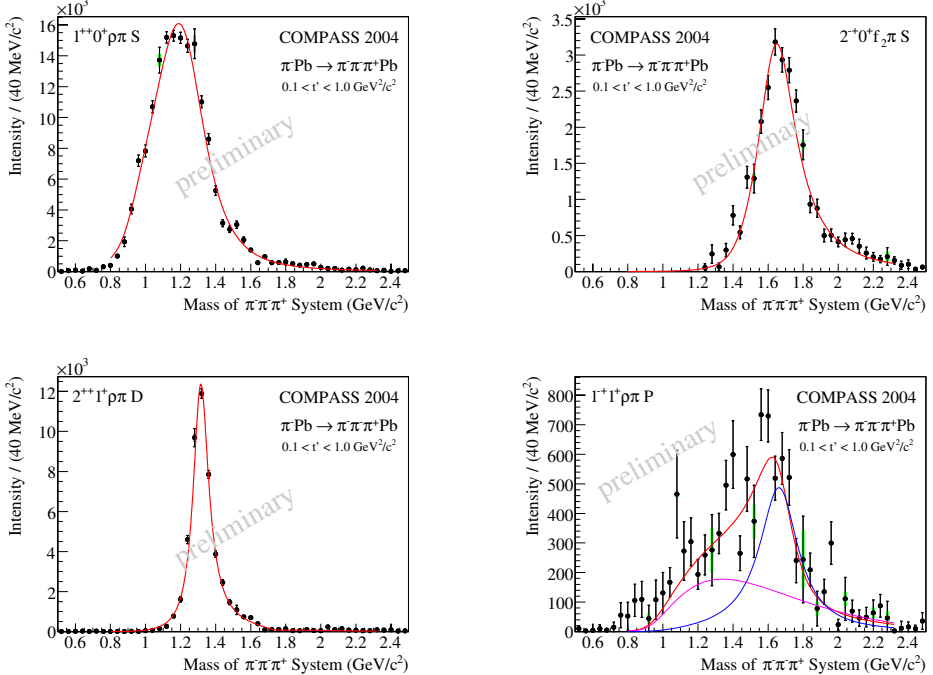
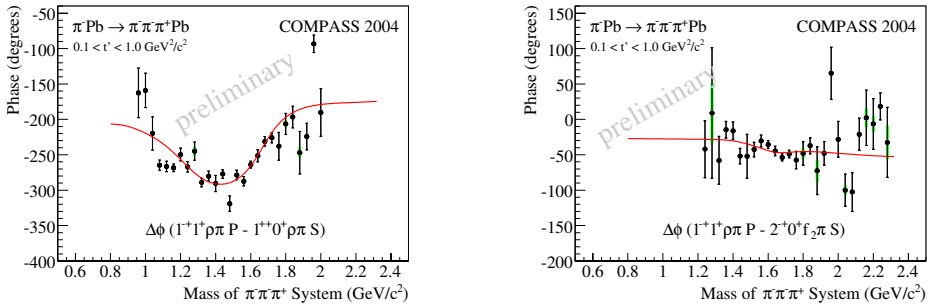


Fig. 4. Intensities of major waves.

Fig. 5. Phase motions of the exotic 1^{-+} wave.

shown in Fig. 5 (left), clearly shows a rising motion around $1.6 \text{ GeV}/c^2$. As the $a_1(1260)$ is no longer resonating at this mass, this observation can be regarded as an independent verification of the resonating nature of the 1^{-+} wave. The parameters deduced for the $\pi_1(1600)$ from our fit are a mass of $M = 1.660 \pm 0.010^{+0.000}_{-0.064} \text{ GeV}/c^2$, and a width of $\Gamma = 0.269 \pm 0.021^{+0.042}_{-0.064} \text{ GeV}/c^2$, where the first uncertainty corresponds to the statistical error, the second to the systematic error, which was estimated by testing the stability of the result with respect to various assumptions

made in the analysis, e.g. adding or removing certain waves, varying cuts or initial parameters for the fit.

In addition to the Breit-Wigner resonance at $1.6 \text{ GeV}/c^2$, represented by the blue line in Fig. 4 (bottom right), the intensity of the 1^{-+} wave has a shoulder at lower masses. In our "standard" fit this shoulder is described by a non-resonant background (purple line), possibly caused by a Deck-like effect. In order to study the systematic error and the stability of the $\pi_1(1600)$, we also tried to include a $\pi_1(1400)$ into the fit, but with parameters fixed to PDG values. This did not alter significantly the intensity at $1.6 \text{ GeV}/c^2$ or the phase motions of the 1^{-+} wave. The fit becomes unstable, however, when a second resonance with free parameters is added in order to describe the low-mass bump. We attribute this to the fact that the $\pi_1(1400)$, if present at all, couples only weakly to the $\pi^- \pi^- \pi^+$ final state. In fact the $\pi_1(1400)$ has been dominantly observed in the $\eta\pi$ channel in the past, and not in the $\pi^- \pi^- \pi^+$ channel. Our statistics at low masses in the $\pi^- \pi^- \pi^+$ channel is not enough to claim or disprove a 1^{-+} resonance at $1.4 \text{ GeV}/c^2$.

In contrast to this, the intensity of the $\pi_1(1600)$ resonance is significant: it corresponds to $\sim 16\%$ of the $\pi_2(1670)$ intensity with a significance of 8 sigma. An incomplete acceptance of the spectrometer not properly taken into account in the Monte Carlo simulation or an incomplete set of waves may introduce leakage of non-exotic waves into the 1^{-+} wave. In order to study this effect, Monte Carlo events were generated using the parameters of 16 dominant waves, excluding the 1^{-+} , which were determined in a mass-dependent fit, and simulating the decay patterns of the corresponding decay channels. Performing the same PWA for the Monte Carlo data as for the real data it was found that the amount of 'fake' intensity in the exotic 1^{-+} wave in the Monte Carlo case is less than 5%, and thus negligible.

5. COMPASS Hadron Run 2008

From 2008 onward, COMPASS is dedicated to precision spectroscopy of mesons using the techniques explained in Sec. 3. A number of new detectors has been installed in order to optimise the setup. These include two CEDAR detectors in the beam line to identify beam pions or kaons via Cherenkov radiation, a recoil proton detector consisting of two concentric rings of scintillators surrounding a 40 cm long liquid hydrogen target, a set of silicon microstrip detectors cooled to cryogenic temperatures for improved radiation hardness, five novel GEM detectors with pixel readout for very small area tracking, and 800 radiation-hard Shashlik blocks for the central part of the second electromagnetic calorimeter. With a $190 - 280 \text{ GeV}/c$ positive or negative hadron beam, we expect to increase the presently available world statistics for both diffractive production of the $\pi_1(1600)$ and central production of the $f_0(1500)$ by about a factor of ten within two years of beam time. The meson spectrum in the mass region up to $2.5 \text{ GeV}/c^2$ will be explored with high statistics for the first time. In addition, completely new measurements on diffractive dissociation of kaons or the polarisability of kaons are planned.

6. Summary

COMPASS has started precision spectroscopy in the light meson sector with the goals to search for gluonic excitations like hybrids or glueballs, to settle the properties of disputed states like the $\pi_1(1400)$, $\pi_1(1600)$ or $f_0(1500)$, and to explore with high statistics also the mass region above $2.2 \text{ GeV}/c^2$. Two production mechanisms are available at COMPASS: diffractive dissociation and central production. Both can be studied in parallel using different projectiles like π , K or protons. The detection of final states with both charged and neutral particles with high acceptance and resolution is one of the key advantages of the experiment compared to previous fixed target experiments. A dedicated run in 2008-2009 was preceded by a short pilot run in 2004, where a $190 \text{ GeV}/c \pi^-$ beam was scattered off a Pb target. We have performed a partial wave analysis of data from the reaction $\pi^- N \rightarrow \pi^- \pi^- \pi^+ N'$. All well-known states are observed. In addition, the spin-exotic wave with quantum numbers $J^{PC} = 1^{-+}$ is found to show significant intensity and phase motion in the $\rho\pi$ decay channel at $1.6 \text{ GeV}/c^2$, which is consistent with the highly debated $\pi_1(1600)$ meson.

Acknowledgments

This work is supported by the German Bundesministerium für Bildung und Forschung, the Maier-Leibnitz-Labor der LMU und TU München, the DFG cluster of excellence *Origin and Structure of the Universe*, and CERN-RFBR grant 08-02-91009.

References

1. P. Abbon *et al.*, *Nucl. Instr. Meth. Phys. Res. Sect. A* **577**, 455 (2007).
2. Y. Chen *et al.*, *Phys. Rev. D* **73**, 014516 (2006).
3. C. Amsler *et al.*, *Phys. Lett. B* **353**, 571 (1995).
4. D. Barberis *et al.*, *Phys. Lett. B* **474**, 423 (2000).
5. K.J. Juge, J. Kuti, C. Morningstar, *AIP Conf. Proc.* **688**, 193 (2004).
6. D.R. Thompson *et al.*, *it Phys. Rev. Lett.* **79**, 1630 (1997).
7. V. Dorofeev *et al.*, *AIP Conf. Proc.* **619**, 143 (2002).
8. A. Abele *et al.*, *Phys. Lett. B* **423**, 175 (1998).
9. A. Abele *et al.*, *Phys. Lett. B* **446**, 349 (1999).
10. G.S. Adams *et al.*, *Phys. Rev. Lett.* **81**, 5760 (1998).
11. Y. Khokhlov, *Nucl. Phys. A* **663**, 596 (2000).
12. G.M. Beladidze *et al.*, *Phys. Lett. B* **313**, 276 (1993).
13. E.I. Ivanov *et al.*, *Phys. Rev. Lett.* **86**, 3977 (2001).
14. J. Kuhn *et al.*, *Phys. Lett. B* **595**, 109 (2004).
15. D.V. Amelin *et al.*, *Phys. Atom. Nucl.* **68**, 359 (2005).
16. M. Lu *et al.*, *Phys. Rev. Lett.* **94**, 032002 (2005).
17. A.R. Dzierba *et al.*, *Phys. Rev. D* **73**, 072001 (2006).